Available online at www.sciencedirect.com
SCIENCE DIRECT®
Solar Energy Materials & Solar Cells
ELSEVIER
Solar Energy Materials & Solar Cells 90 (2006) 1555–1578
www.elsevier.com/locate/solmat

Review

Review of the maximum power point tracking algorithms for stand-alone photovoltaic systems

V. Salas*, E. Olías, A. Barrado, A. Lázaro

Departamento de Tecnología Electrónica/Grupo de Sistemas Electrónicos de Potencia, Universidad Carlos III de Madrid, Avda. de la Universidad, 30-28911 Leganés, Madrid, Spain

Received 7 May 2005; accepted 11 October 2005
Available online 10 January 2006

Abstract

A survey of the algorithms for seeking the maximum power point (MPP) is proposed. As has been shown, there are many ways of distinguishing and grouping methods that seek the MPP from a photovoltaic (PV) generator. However, in this article they are grouped as either direct or nondirect methods. The indirect methods (''quasi seeks'') have the particular feature that the MPP is estimated from the measures of the PV generator's voltage and current PV, the irradiance, or using empiric data, by mathematical expressions of numerical approximations. Therefore, the estimation is carried out for a specific PV generator installed in the system. Thus, they do not obtain the maximum power for any irradiance or temperature and none of them are able to obtain the MPP exactly. Subsequently, they are known as ''quasi seeks''.

Nevertheless, the direct methods (''true seeking methods'') can also be distinguished. They offer the advantage that they obtain the actual maximum power from the measures of the PV generator's voltage and current PV. In that case, they are suitable for any irradiance and temperature. All algorithms, direct and indirect, can be included in some of the DC/DC converters, Maximum power point trackings (MPPTs), for the stand-alone systems.

Keywords: Maximum power point; Maximum power point tracking (MPPT); Power electronics; Photovoltaic energy

*Corresponding author. Fax: +34916249430.
E-mail address: vsalas@ing.uc3m.es (V. Salas).

0927-0248/$ - see front matter © 2005 Elsevier B.V. All rights reserved.
doi:10.1016/j.solmat.2005.10.023

Contents

1. Introduction

In the current century, the world is increasingly experiencing a great need for additional energy resources so as to reduce dependency on conventional sources, and photovoltaic (PV) energy could be an answer to that need. PV cells are being used in space and terrestrial applications where they are economically competitive with alternative sources. Furthermore, the PV industry has demonstrated high growth rates over recent years, 30% per year in the late 1990s. By the year 2010, it is assumed that modules will cost 1.50 €/Wp and systems 3.00 €/Wp.

Generally, PV systems can be divided into three categories: stand-alone, grid-connection and hybrid systems. For places that are far from a conventional power generation system, stand-alone PV power supply systems have been considered a good alternative. These systems can be seen as a well-established and reliable economic source of electricity in rural remote areas, especially where the grid power supply is not fully extended. Such systems are presented in two scales: applications at a smaller scale, from 1 to 10 kW, are used to supply electric power in developing countries, the so-called solar home systems, SHS; and stand-alone PV systems of several hundred thousand watts in size, from 10 to 100 kW, on the roofs of dwellings. In general, they have the advantages of using a simple system configuration and simple control scheme. For our study, only DC loads will be considered. Typical DC voltage levels are 12, 24, 48 and 60 V.

In those systems, the performance of a PV system relies on the operating conditions. Then, the maximum power extracted from the PV generator depends strongly on three factors: insolation, load profile (load impedance) and cell temperature (ambient temperature), assuming a fixed cell efficiency.

The variation of the output I–V characteristic of a commercial PV module as a function of temperature and irradiation is shown in Figs. 1–4. It can be observed that the temperature changes mainly affect the PV output voltage, while the irradiation changes mainly affect the PV output current.

Nevertheless, PV systems should be designed to operate at their maximum output power levels for any temperature and solar irradiation level at all times. The last significant factor, which determines the PV throughput power, is the impedance of the load. In our case, this

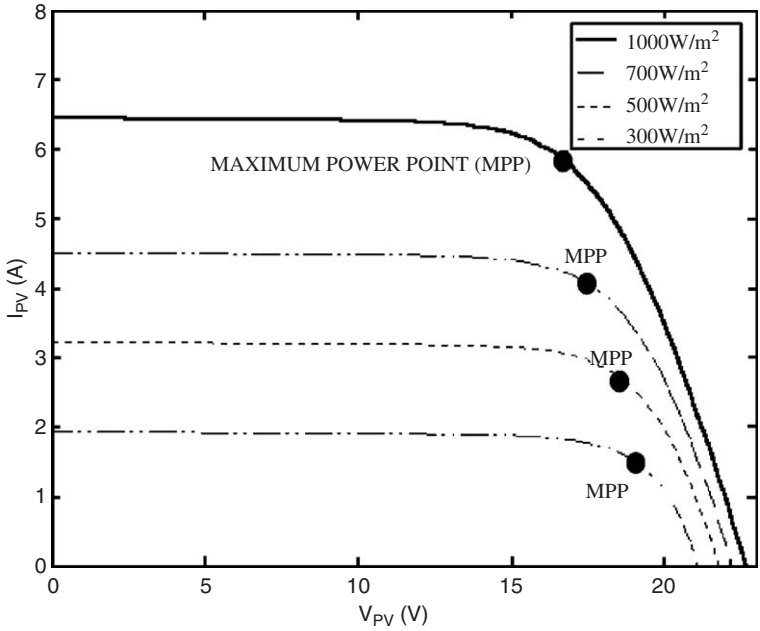

Fig. 1. *I–V* photovoltaic characteristic for four different irradiation levels.

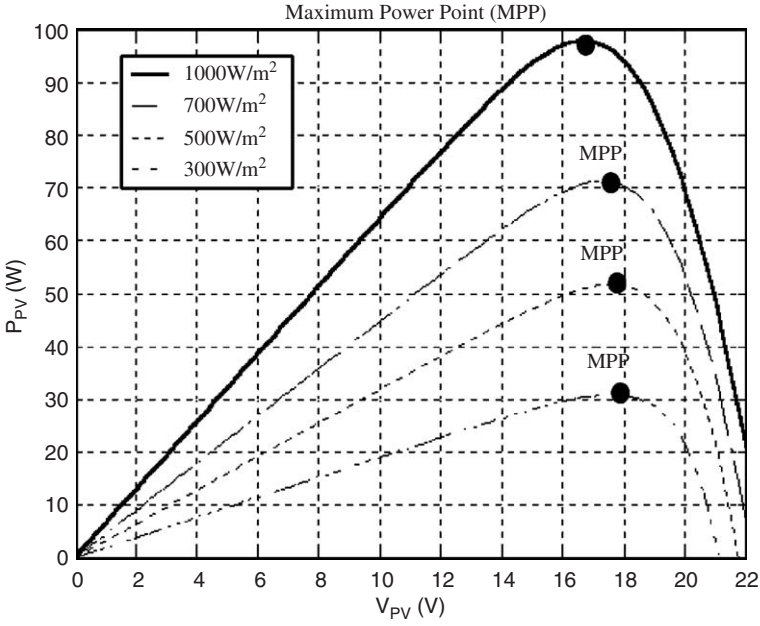

Fig. 2. *P–V* photovoltaic characteristic for four different irradiation levels.

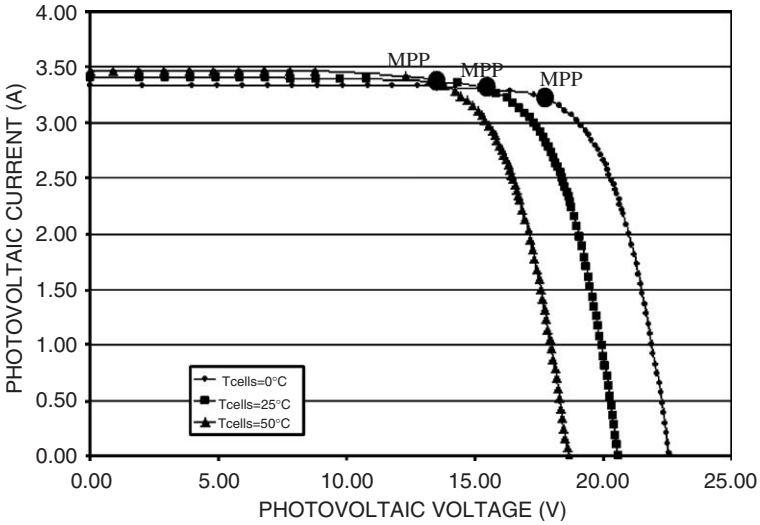

Fig. 3. *I–V* characteristics for three temperatures level.

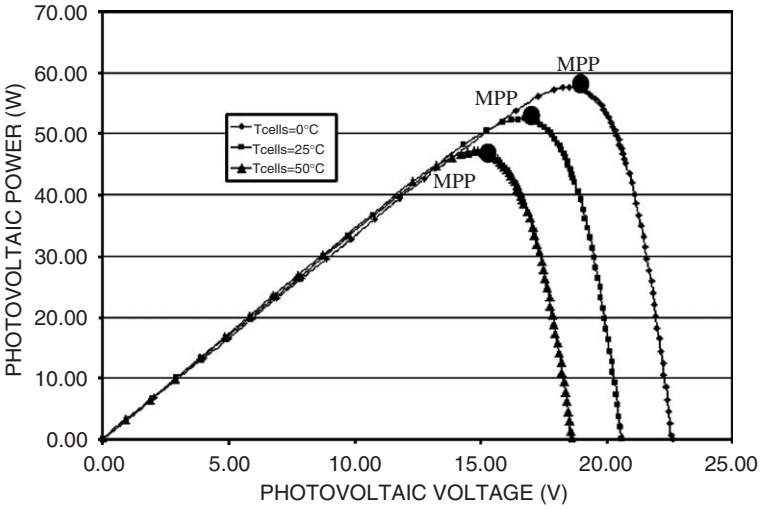

Fig. 4. *P–V* characteristic for three temperatures level.

consists of a DC load and batteries. However, it should be noted, that such impedance is not constant. When a PV generator is directly connected to the load, the system will operate at the intersection of the *I–V* curve and load line, which can be far from the maximum power point (MPP).

The maximum power production is based on the load-line adjustment under varying atmospheric conditions.

Another important element of a stand-alone PV system is the battery because of the fluctuating nature of the output delivered by the PV array [1]. Moreover, the load, in many cases, requires a power level that is maintained constant. Commonly, lead-acid batteries

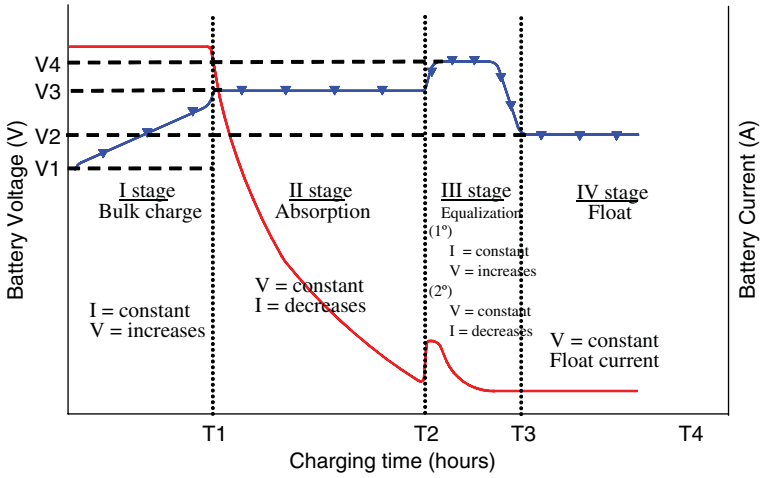

Fig. 5. General four step charging battery algorithm.

are used, because of their wide availability in many sizes, their low cost and their well-understood performance characteristics.

Thus, in most cases, a charge controller is an essential element [2], except in small systems with well-defined loads, using low voltage "self-regulating modules" or using a large battery or small array. If finally, a battery charge is used, it will control the voltage and charge current that is applied to the battery in order to protect it from being over charged, over discharged and from load control functions.

Depending on the level of sophistication in the charger technology, different charge algorithms are presented, i.e., a collection of controls over electrical parameters and a timing, associated with multiple voltage and current levels, applied sequentially to the charging system hardware for the express purpose of recharging the battery appropriately. Generally, battery manufacture refer to four distinct charging modes, or stages, within a battery charging cycle, Fig. 5: bulk, absorption, equalization and float. However, not all battery chargers have the four stages.

The previous charging modes can be implemented in several possible ways. The most common controller topologies for battery charge regulation are shunt and series type configuration. The point is that in the two topologies, time after time, PV panels are usually forced to operate at the battery voltage. This is almost always below the peak power point, so some of the power generating capability is lost.

In order to overcome the undesired effects on the output PV power and draw its maximum power, it is possible to insert a DC/DC converter between the PV generator and the batteries, which can control the seeking of the MPP, besides including the typical functions assigned to the controllers. These converters are normally named as maximum power point trackers (MPPTs). They consist of a topology and control circuit where there will be a MPP seeking algorithm. As Fig. 6 shows, the input DC–DC converter part is formed by the PV array and the output section by the batteries and load. The role of the MPPT is to ensure the operation of the PV generator at its MPP, extracting the maximum available power.

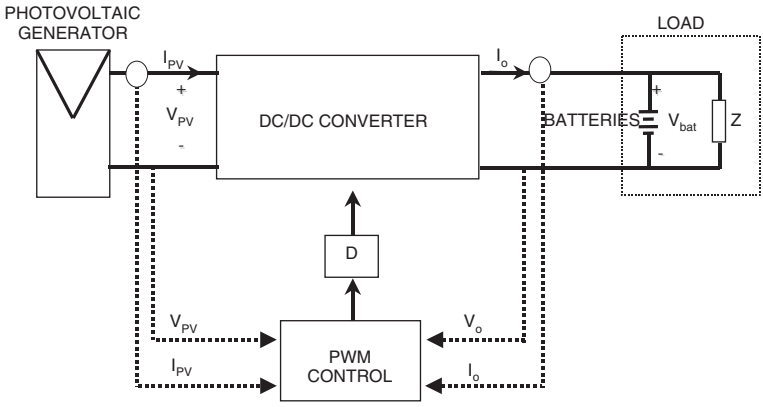

Fig. 6. General block diagram of a stand-alone PV system with MPPT.

Table 1
Possible variables for controlling in a DC/DC converter

Variables		
V_{PV}	Output voltage photovoltaic generator	Input voltage DC/DC converter
I_{PV}	Output current photovoltaic generator	Input current DC/DC converter
V_o		Output voltage DC/DC converter
I_o		Output voltage DC/DC converter

However, their losses have to be small enough to improve the efficiency of the overall system. This could increase the gap between the PV peak power voltage and the voltage at which they are forced to operate in a system without a peak power tracking. Theoretically, it is foreseeable that a MPPT would yield the most impressive gains in cold weather because that would raise the PV array' peak power voltage point well above the usual battery operating voltage.

Fig. 6 shows the general block diagram for a charge batteries system, with MPPT, using a generic DC/DC converter. This one is connected to the PV generator, a battery and a load profile (such as a resistance, DC/DC motor…).

The main objective is to obtain the maximum power from the PV generator for the first-load batteries stage. That is to say, when the batteries are fully or partially discharged, in some state of charge less than 100%, then it is necessary to control one/or some of the input/output following variables; Table 1.

2. Seeking algorithms classification

The first methods, used in aerospace applications, date from the 1970s, in companies or research centres such as Honeywell Inc. or NASA [3–9]. The methods developed up until now can be grouped by their different parameters. If they are grouped according to the control variables involved (measured) in the seeking process they can be differentiated by two variable and one variable methods.

The two variables methods use the voltage measurements, V_{PV}, and current, I_{PV} of the PV output power. Among others, the differentiation, perturbation and observation (P&O) and the conductance incremental (C.I.) methods can be cited.

On the other hand, methods using one variable control can be distinguished as well. Pertaining to this group are the feedback voltage, open-voltage PV generator, open-voltage PV cell as well as the short circuit current method.

Other classifications can be based on the function of the methods or control strategies used. Thus, two categories can be presented: direct and indirect methods. This classification, therefore, will be presented in this paper, and will be developed in detail in the rest of this article.

2.1. The indirect control: the "quasi seeking"

The indirect methods are based on the use of a database that includes parameters and data such as, for instance, curves typical of the PV generator for different irradiances and temperatures, or on the use of the mathematical functions obtained from empirical data to estimate the MPP. In most cases a prior evaluation of the PV generator is then required, or else it is based on the mathematical relationship obtained from empirical data, which does not meet all climatologic conditions. The following methods belong to this category: curve-fitting, look-up table, open-voltage PV generator, short circuit PV generator and the open-circuit cell. These will be studied next in greater detail.

2.1.1. Curve-fitting method

The nonlinear characteristic of PV generator can be modelled off-line, from conventional single-diode, two-diode and modified two diode model, using mathematical equations or numerical approximations [10,11]. However, their resolution is impossible by analogue control and very difficult by conventional digital control. Hence, their application does not seem suitable for obtaining the MPP. Nevertheless, other model-based approaches can be used [12–14]. In consequence, for instance, according to Ref. [14], Eq. (1) is the P–V characteristic of a PV generator, where a, b, c and d are coefficients determined by the sampling of m values of PV voltage, V_{PV}, PV current, I_{PV}, and PV power, P_{PV}, in the required interval. Thus, the voltage at which the maximum power becomes maximum is obtained by means of Eq. (2).

$$P_{PV} = aV_{PV}^3 + bV_{PV}^2 + cV_{PV} + d, \tag{1}$$

$$V_{MPP} = -b\sqrt{b^2 - 3ac}/3a. \tag{2}$$

This process should be repeated every few milliseconds in order to find a fine MPP. The accuracy will depend on the number of samples.

The disadvantage of this method is that either it requires accurate knowledge of the physical parameters relating to the cell material and manufacturing specifications or the expressions used are not valid for all climatological conditions. In addition, it might require a large memory capacity for calculation of the mathematical formulations.

2.1.2. Look-up table method

In this case, the measured values of the PV generator's voltage and current are compared with those stored in the control system, which correspond to the operation in the maximum point [15], under concrete climatological conditions. Then, this algorithm has as the disadvantage that a large capacity of memory is required for storage of the data. Moreover, the implementation must be adjusted for a panel PV specific. In addition, it is difficult to record and store all possible system conditions.

2.1.3. Open-circuit voltage photovoltaic generator method

This algorithm, used in Refs. [16–20], is based on the voltage of PV generator at the MPP which is approximately linearly proportional, k_1, to its open-circuit voltage, V_{oc}. The proportional constant depends on the fabrication technologies solar cells technology, fill factor and the meteorological conditions, mainly.

$$k_1 = \frac{V_{MPP}}{V_{OC}} \cong \text{Constant} < 1. \tag{3}$$

This property can be implemented by means of the flow chart shown in Fig. 7. Thus, the PV generator's open-circuit voltage is measured by interrupting the normal operation of the system, with a certain frequency, storing the measured value. Later, the MPP is

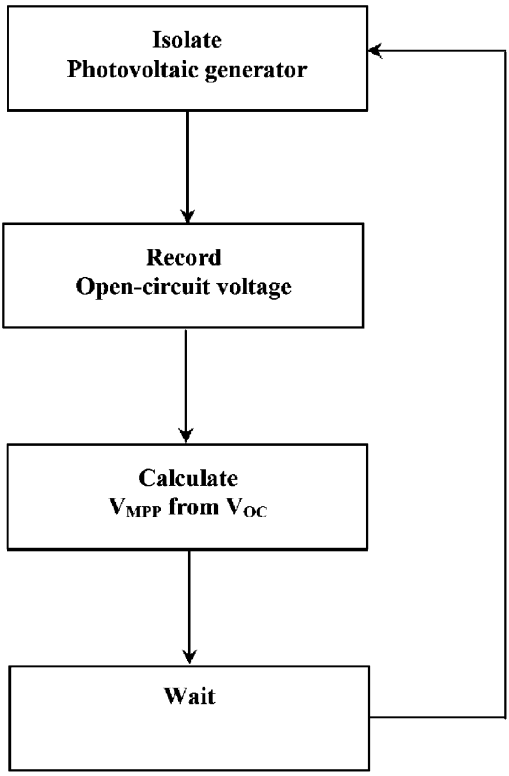

Fig. 7. Open-circuit voltage photovoltaic generator algorithm flowchart.

calculated, according to Eq. (3), and the operation voltage is adjusted to the maximum voltage point. This process will be repeated periodically. Although this method is apparently simple, it is difficult to choose an optimal value of the constant K_1. However, the literature [20–22], reports K_1 values ranging from 0.73 to 0.80, for polycrystalline PV modules, as well as a typical interval of sampling of 15 ms [20].

Since adjustment of the reference voltage of V_{oc} is chosen as a fixed fraction, assuming that it remains constant for a wide variation of temperature and insolation, and does not change appreciably, with the aging of the array, this method cannot be integrated in one of the 'true seeking methods' of the MPP. The exactitude of the adjustment of the voltage operation to the maximum voltage, V_{MPP}, depends on the choice of this fraction, compared with the real relation that exists between V_{MPP} and V_{oc}.

Hence, this method has as an advantage that it is simple and low-priced. It uses only one feedback loop. Nevertheless, its drawback is that the interrupted system operation yields power losses when scanning the entire control range. Thus, the real power extracted is not considered to be of (from) the panels. That is, as it is assumed that for given open-circuit voltage the maximum point is determined if the operation point is incorrect, or slightly inexact, the extracted power will not be the maxima.

2.1.4. Short-circuit photovoltaic generator method

A method similar to the above procedure is used in Refs. [23,24]. In this case, it is based on the empirical fact of a linear dependency between the current in the MPP and that of a short-circuit current, thus fulfilling relationship (4). As does the previous method, the proportional constant depends on the fabrication technologies solar cells technology, fill factor and the meteorological conditions, mainly. However, for this method, for polycrystalline PV modules, the constant, k_2, can be considered to be around 0.85.

$$k_2 = \frac{I_{PMP}}{I_{SC}} \cong \text{Constant} < 1. \tag{4}$$

However, in many cases, the way of determining k_2 is more complicated than only a fixed value, as in Ref. [24]. In that paper, a PV scanning is performed every several minutes in order to calculate k_2. After k_2 is obtained, the system remains with the approximation (4), until the next calculation of k_2.

The flow chart of the control is then, similar to the open-circuit voltage method. Therefore, this method offers the same advantages and disadvantages as the above control.

2.1.5. Open-circuit voltage photovoltaic test cell method

In order to avoid possible drawbacks related to the frequent interruption of the system, Refs. [6,25–28] proposed, as an alternative, an additional use of a cell test. Thus, the PV generator's open-circuit voltage is measured from the single cell, which is electrically independent from the rest of the PV array. The resulting values of the K_3 will be applied to the main PV generator.

$$k_3 = \frac{V_{MPP}}{V_{OC,\ \text{cell test}}} \cong \text{Const} < 1. \tag{5}$$

This method's advantage is that it is simple and economical; it uses only one feedback-loop control. Moreover, it avoids the problems caused by the interruptions of the operation of the PV set out in the previous method.

As a disadvantage, it supposes that the test cell has properties identical to each cell of the PV generator main. Therefore, V_{oc} of the test cell is considered proportional to V_{oc} of the PV unit used in the selection of the MPP. If the supposition is incorrect, maximum power will not be extracted. And, finally, it can be an unsuitable method for applications with surface limitations (i.e. solar vehicles).

2.2. Direct control: the "true seeking"

Direct methods include those methods that use PV voltage and/or current measurements. From those, and taking into account the variations of the PV generator operating points, the optimum operating point is obtained. These algorithms have the advantage of being independent from the a priori knowledge of the PV generator characteristics. Thus, the operating point is independent of isolation, temperature or degradation levels. The problems are undesirable errors which strongly affect tracker accuracy. The methods belonging to this group include the differentiation, feedback voltage (current), P&O, C.I., auto-oscillation as well as the fuzzy logic, among others. Other types of classification, which distinguish between sample and modulation methods, can be included within this group.

2.2.1. Sampling methods

In these procedures, a sample is made of the PV's generator voltage and current. Afterwards, using diverse strategies, in every sampling, the PV output power, P_{PV} (t) is gathered. Such sampling has as an objective for the determining of the relative time evolution of the abovementioned variable. So, firstly, the $P_{PV}(t)$ is computed. At a stage two, the PV power $P_{PV}(t+\Delta t)$ is computed again. After gathering the past and the present information on the P_{PV}, the controller makes a decision depending on the location of the operating point. This tracking process repeats itself indefinitely until the peak power point is reached. In accordance with this principle, the following methods can be distinguished.

2.2.1.1. Differentation method. This technique is presented in Refs. [29,30], and is based on the property in which the MPP is located by solving Eq. (6).

$$\frac{dP_{PV}}{dt} = V_{PV}, \quad \frac{dI_{PV}}{dt} + I_{PV}\frac{dV_{PV}}{dt} = 0. \tag{6}$$

However, in order to provide real time adjustments of the operating point, this equation must be solved quickly. This is difficult because solving this equation requires, at least, eight calculations and measurements: a determination of present array voltage V_{PV}; a determination of present array current I_{PV}; a measure of the change in voltage, dV_{PV}, in the face of a given operating point perturbation (dt); a measure of the change in current, dI_{PV}, corresponding to the operating point perturbation; a calculation of the product V_{PV} times dI_{PV}; a calculation of the product I_{PV} times dV_{PV}; a calculation of the resulting sum $V_{PV}\,dI_{PV} + I_{PV}\,dV_{PV}$; and a comparison of this sum to an equal perturbation on the opposite side of the operating point or the operating point power. Furthermore, if the final sum is not zero, a ninth determination must be made of the sign of the dP_{PV} sum. This sign indicates the direction that the operating point must be adjusted to reach the MPP.

2.2.1.2. Feedback voltage (current) method. If there is no battery present in the system, in order to tie the bus voltage at a nearly constant level, a simple control can be applied, as in Refs. [31,32]. Thus, the feedback of the PV voltage (current) and the comparison with a constant voltage (current) can be used to continuously adjust the duty cycle (D) of a DC/DC converter, to operate the PV panel at a predefined operating point, close to the MPP, Fig. 8.

The disadvantages of this configuration are the same as for the method of direct connection (PV generator + load profile). That is, the system is not able to adapt to changeable environmental conditions, such as irradiance and temperature. However, if batteries are present in the system, a common technique is to compare with a reference constant voltage, where it is assumed that it corresponds to the V_{MPP}, under environmentally specific conditions. The resultant signal differentiation (error signal) is used to control the DC/DC converter.

Although the implementation of this variant is not relatively simple, it fails as well to fulfil the proposed objective because it does not take into account the effects of irradiation and temperature variations.

The advantages of this method are the same as the previous methods: it is a simple and economical method and uses only one feedback-loop control. Nevertheless, as has been mentioned before, it presents the following disadvantages: it cannot be applied in a generalized fashion in systems which do not consider the effect of variations of the irradiation and temperature of the PV panels. It cannot be applied to the systems with batteries.

2.2.1.3. Perturbation and observe (''P&O'') method. The ''P&O'' method is that which is most commonly used in practice by the majority of authors [33–38], among others. It is an iterative method of obtaining MPP. It measures the PV array characteristics, and then perturbs the operating point of PV generator to encounter the change direction. The

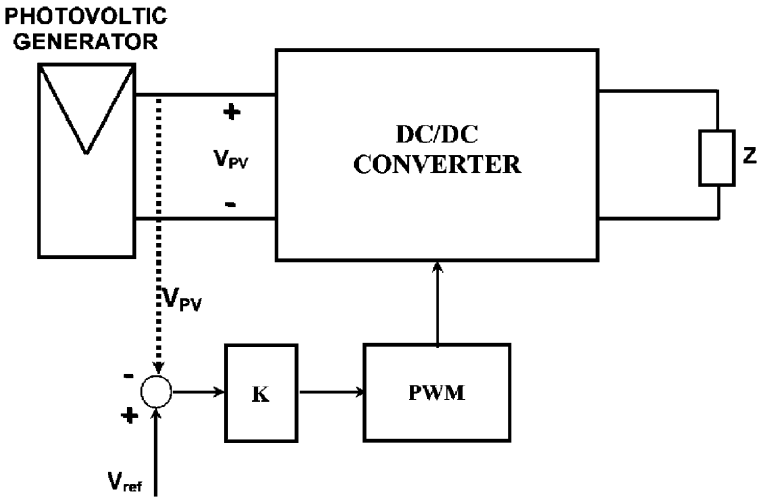

Fig. 8. Voltage-feedback with PWM modulation.

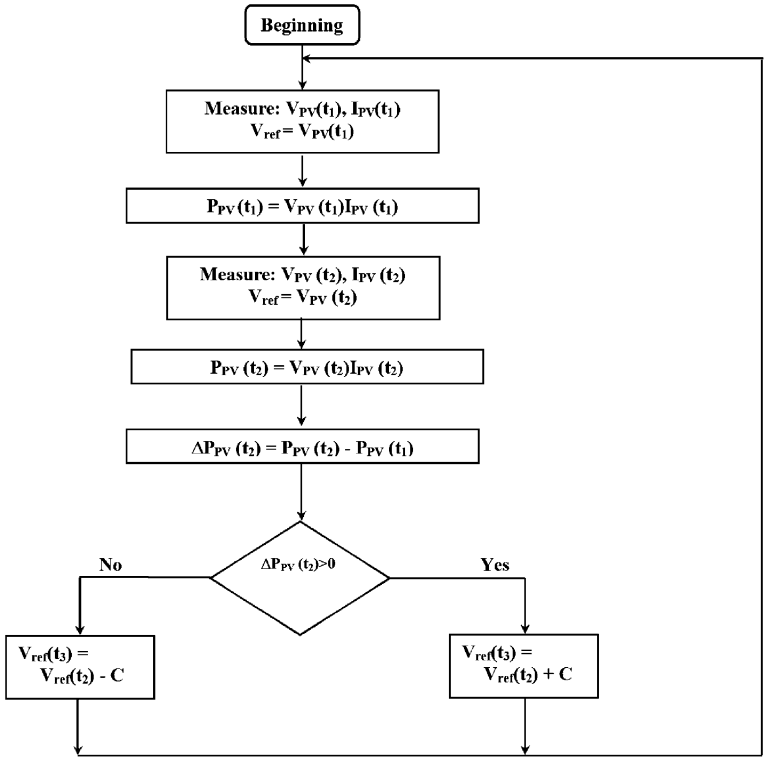

Fig. 9. Conventional Perturbation and Observe algorithm flowchart. C is the step of the perturbation.

Table 2
True table associated with the operation for the Perturbation and Observe (P&O) method

$\Delta P_{PV}(t_2)$	$V_{PV}(t_3)$
>0	+
<0	−

The "+"sign refers to an increment and "−" sign to a decrease.

maximum point is reached when $dP_{PV}/dV_{PV} = 0$. There are many varieties, from simple to complex. An example algorithm flowchart of the most basic form is shown in Fig. 9.

Doing this, the operating voltage of the PV generator is perturbed, by a small increment ΔV_{PV}, and the resulting change, ΔP_{PV}, in power, is measured. If ΔP_{PV} is positive, the perturbation of the operating voltage should be in the same direction of the increment. However, if it is negative, the system operating point obtained moves away from the MPPT and the operating voltage should be in the opposite direction of the increment. The logic of this algorithm is explained in Table 2 and Fig. 9. In addition, Fig. 10 shows possible implementation.

In accordance with Table 2, if the PV power has increased, the operating point should be increased as well. However, if the PV power has decreased, the voltage should do the same.

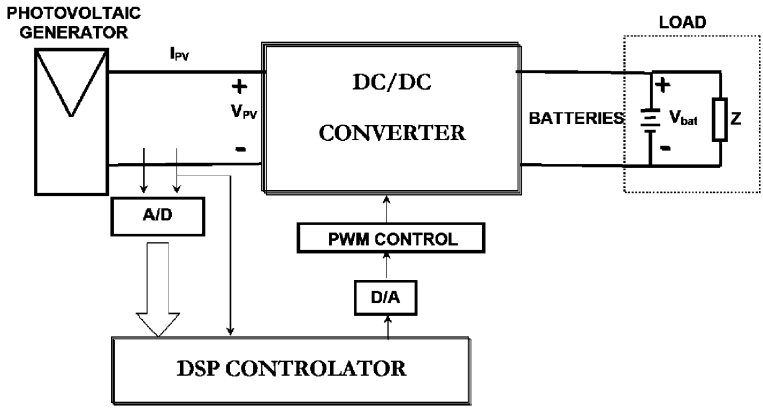

Fig. 10. Example Perturbation and Observe implementation system [37].

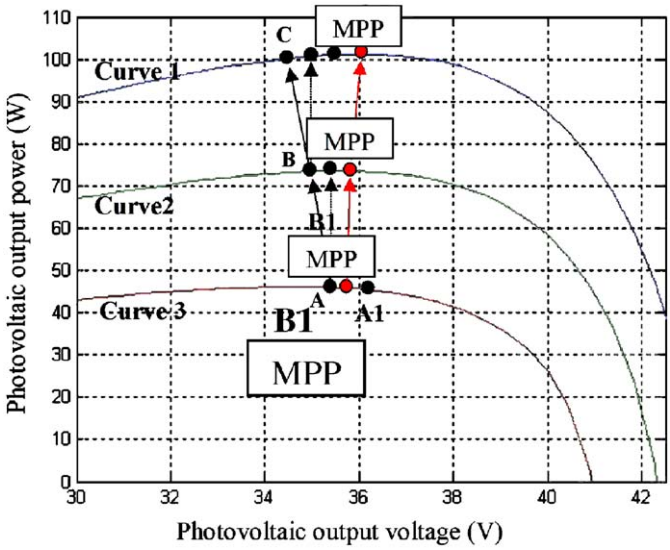

Fig. 11. Deviation from the MPP with the Perturbation and Observation algorithm under rapidly changing insolation levels [39,40].

Nevertheless, a disadvantage of this method, described by Hussein et al. [39], appears in the case of a sudden increase of irradiance, Fig. 11, where the algorithm reacts as if the increase occurred as a result of the previous perturbation of the operating voltage.

In order to better understand this phenomenon, see Fig. 11. Thus, the case is considered in which the irradiance is such that it generates the P–V curve characteristics, curve 1. In this way, the operating voltage initially oscillates around the maximum point, from A to A1. Now, an increase in the power will be measured because the solar irradiation has increased from curve 1 to curve 2. Then, if one assumes that being in point A, that it comes from a diminution of the voltage, and before the following disturbance takes place, the

irradiance is increased, with the curve characteristic being now curve 2, and the operation point will occur at B1. Indeed, since there has been a positive increase in power, the disturbance will continue in the same direction, see Table 2. In other words, the voltage will diminish and go to point B. Furthermore, if the irradiance is increased again quickly to curve 3, there will be another increase in positive power, with which the operation point will now be C. That is, due to two increases of irradiance, the operation point has been transferred from A to C, moving away from the maximum point. This process remains until the increase of the irradiance slows or stops.

The advantages of this method can be summarized as follows: a previous knowledge is not required of PV generator characteristics; it a relatively simple method. Nevertheless, in their most simple form, at a steady state, the operating point oscillates around the MPP, giving rise to the wasting of some amount of available energy. In addition, it is an unsuitable method with rapidly changing atmospheric conditions [39]. However, their reaction can be improved by increasing the speed of the execution of the control algorithm or introducing an optimization [41,42].

2.2.1.4. Conductance incremental method ("C.I."). An alternative to the "P&O" method was proposed by Hussein et al. [39], developing the "C.I." method. It is based on Eq. (7). That is, differentiating the PV power with respect to voltage and setting the result to zero, Fig. 12.

$$\frac{dP_{fv}}{dV_{fv}} = I_{fv}\frac{dV_{fv}}{dV_{fv}} + V_{fv}\frac{dI_{fv}}{dV_{fv}} = I_{fv} + V_{fv}\frac{dI_{fv}}{dV_{fv}} = 0, \tag{7}$$

$$-\frac{I_{fv}}{V_{fv}} = \frac{dI_{fv}}{dV_{fv}}. \tag{8}$$

The left-hand side of Eq. (8) represents the opposite of the instantaneous conductance, $G = I_{PV}/V_{PV}$, whereas the right hand side of the Eq. (8) represents its incremental conductance. On the other hand, the incremental variations, dV_{PV} and dI_{PV}, can be approximated by the increments of both the parameters, ΔV_{PV} and ΔI_{PV}, with the aim of measuring the actual value V_{PV} and I_{PV} with the values measured in the previous instant, expressions (9) and (10), respectively.

$$dV_{PV}(t_2) \approx \Delta V_{PV}(t_2) = V_{PV}(t_2) - V_{PV}(t_1), \tag{9}$$

$$dI_{PV}(t_2) \approx \Delta I_{PV}(t_2) = I_{PV}(t_2) - I_{PV}(t_1). \tag{10}$$

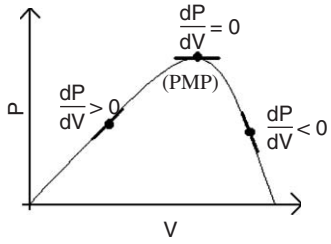

Fig. 12. Characteristics curve of the P–V photovoltaic generator. Variation of the dP/dV.

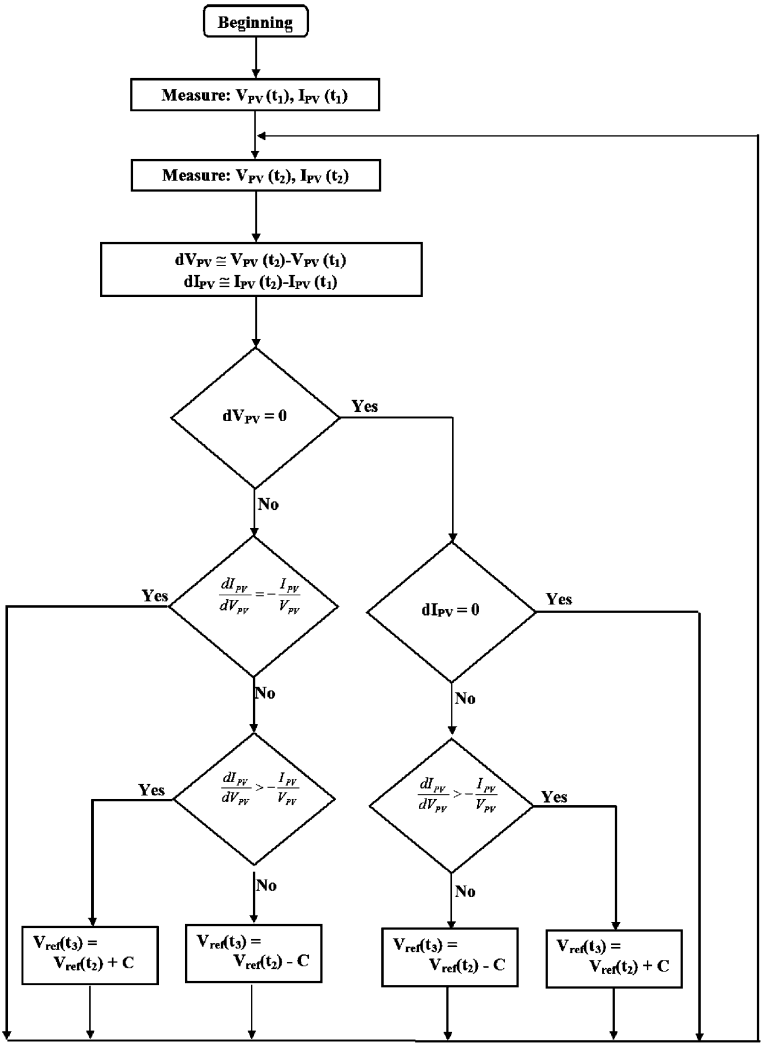

Fig. 13. Incremental conductance algorithm flowchart.

Therefore, analyzing the derivative one can test whether the PV generator is operating at its MPP or far from it, Eqs. (11)–(13), Fig. 13. In addition, Fig. 14 shows, as an example, the flowchart implemented by Hussein et al. [39].

$$\frac{dP_{PV}}{dV_{PV}} > 0 \quad \text{for} \quad V_{PV} < V_{PMP}, \tag{11}$$

$$\frac{dP_{PV}}{dV_{PV}} = 0 \quad \text{for} \quad V_{PV} = V_{PMP}, \tag{12}$$

$$\frac{dP_{PV}}{dV_{PV}} < 0 \quad \text{for} \quad V_{PV} > V_{PMP}. \tag{13}$$

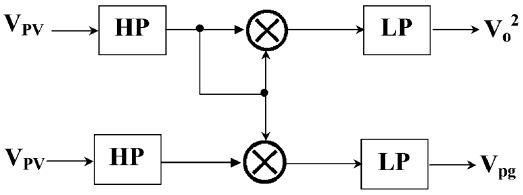

Fig. 14. Circuitry used to implement the parasitic capacitance method.

The main advantage of this algorithm is that it offers a good yield method under rapidly changing atmospheric conditions. Also, it achieves lower oscillation around the MPP than the P&O method, even though, when the P&O method is optimized, the MPPT efficiencies of the incremental conductance and P&O MPPT algorithms are, essentially, the same [40,41]. Nonetheless, it has as drawback that it requires complex control circuit which might have resulted in a high cost system 10 years ago. However, today there are many options for doing it much more cheaply.

2.2.1.5. Parasitic capacitance method. This method was developed by Branbrilla et al. [43], and is similar to the incremental conductance method, except that the effect of the PV cell's parasitic union capacitance, c_{PV}, is included. The analysis is carried out with Eq. (14), instantaneous PV output power, where $P_{PV}(t)$, $I_{PV}(t)$ and $V_{PV}(t)$ are the current and voltage in the time function, respectively.

$$P_{PV}(t) = I_{PV}(t)V_{PV}(t). \tag{14}$$

Then, if the current can be expressed as a time function, $V_{PV}(t)$, the power can be obtained by means of the expression (15).

$$P_{PV}(t) = F(V_{PV}(t))V_{PV}(t). \tag{15}$$

Then, the condition of the MPP is fulfilled for Eq. (16).

$$\frac{dP_{PV}(t)}{dV_{PV}(t)} = \frac{dF(V_{PV}(t))}{dV_{PV}(t)} + F(V_{PV}(t)) = 0. \tag{16}$$

That is, relation (17) is fulfilled.

$$g_p - g_i = 0, \tag{17}$$

where g_p (the incremental conductance) and g_i (instantaneous conductance) are defined by means of Eqs. (18) and (19), respectively. Later, applying the rule of the chain to g_p it can be expressed according to Eq. (20).

$$g_p = \frac{dF(V_{PV}(t))}{dV_{PV}(t)}, \tag{18}$$

$$g_i = -F(V_{PV}(t)), \tag{19}$$

$$g_p = \frac{dF}{dt}\frac{dt}{dV_{PV}}. \tag{20}$$

In this way, the Eq. (16) can be rewritten as Eq. (21).

$$\dot{I}_{\mathrm{PV}}(t)V_{\mathrm{PV}}(t) + I_{\mathrm{PV}}(t)\dot{V}_{\mathrm{PV}}(t) = 0. \tag{21}$$

Assuming that relation (22) is fulfilled, the power can now be expressed according to expression (23). Then, the maximum power is transferred when Eq. (24) is suited, where the dot represents the first derived and both dots the second derived.

$$I_{\mathrm{PV}}(t) = F(V_{\mathrm{PV}}(t)) + c_{\mathrm{PV}}\dot{V}_{\mathrm{PV}}(t) = 0, \tag{22}$$

$$P_{\mathrm{PV}}(t) = [F(V_{\mathrm{PV}}(t)) + c_{\mathrm{PV}}\dot{V}_{\mathrm{PV}}(t)]V_{\mathrm{PV}}(t), \tag{23}$$

$$\frac{\mathrm{d}F(V_{\mathrm{PV}}(t)))}{\mathrm{d}V_{\mathrm{PV}}(t)} + C_{\mathrm{p}}\left(\frac{\ddot{V}_{\mathrm{PV}}(t)}{\dot{V}_{\mathrm{PV}}(t)} + \frac{\dot{V}_{\mathrm{PV}}(t)}{V_{\mathrm{V}}(t)}\right) - \frac{F(v_{\mathrm{p}})}{v_{\mathrm{p}}} = 0, \tag{24}$$

$$I_{\mathrm{PV}}(t) = I_{\mathrm{PV,cc}} + \sum_{1}^{\infty} a_n^I \cos(n\omega_{\mathrm{o}}t) + b_n^I \sin(n\omega_{\mathrm{o}}t), \tag{25}$$

$$V_{\mathrm{PV}}(t) = V_{\mathrm{PV,cc}} + \sum_{1}^{\infty} a_n^V \cos(n\omega_{\mathrm{o}}t) + b_n^V \sin(n\omega_{\mathrm{o}}t), \tag{26}$$

$$P_{\mathrm{PV}} = V_{\mathrm{PV,cc}}I_{\mathrm{PV,cc}} + \frac{1}{2}\sum_{1}^{\infty} a_n^I a_n^V + b_n^I b_n^V. \tag{27}$$

In addition, the three terms of Eq. (24) represent the instantaneous conductance, incremental conductance and the induced ripple from the parasitic capacitance, respectively. The first and second derivatives take into account the AC ripple components generated by the converter. If c_{PV} is equal to zero then expression (24) simplifies the incremental conductance method.

$$g_{\mathrm{p}} = \frac{P_{\mathrm{gp}}}{V_{\mathrm{o}}^2} = \frac{\frac{1}{2}\sum_{n=1}^{\infty}[a_n^i a_n^v + b_n^i b_n^v]}{\frac{1}{2}\sum_{n=1}^{\infty}[(a_n^v)^2 + (b_n^v)^2]}. \tag{28}$$

The array differential conductance can be obtained by Eqs. (25)–(28), where P_{gp} is the average ripple power, V_{o} the voltage ripple and $a_n^i, a_n^v, b_n^i, b_n^v$ are the coefficients of the Fourier series of the PV voltage and current ripple. In addition, the values of P_{gp} and V_{o}^2 can be obtained in accordance with Fig. 14, which is the diagram used for the implementation of this method. The two band-pass filters, HP, remove the continuous component of V_{PV} and I_{PV}, retaining ripple components. Finally, the two low-pass filters, LP, remove the components in high frequency and retain only the continuous component, such as P_{gp} and V_{o}^2, with which g is obtained, Eq. (28). This can be used until it has fulfilled the expression (17).

The disadvantage of this method is that it requires two multiplications with the following complexity of the control circuit.

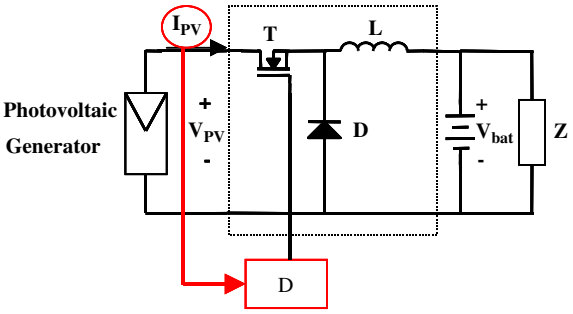

Fig. 15. Block diagram of a stand-alone PV system with the only current PV algorithm [44].

2.2.1.6. The only current photovoltaic method. Up to now, in the direct methods the PV voltage and current have been measured. However, it is possible to find a method that only uses the PV current [44,45], based on the Fig. 15.

The nonlinear PV array can be modelled [11] as $I_{PV} = f(V_{PV}, I_{PV})$, Eq. (29), where I_{PV} = operating current PV; V_{PV} = operating voltage PV; R_s = cell series parasitic resistance; R_P = cell shunt parasitic resistance; m = junction constant; and I_0 = cell reverse saturation current; I_L = cell photocurrent. Then, it can be rearranged to obtain I_{PV} as a sole function of V_{PV}, $I_{PV} = f(V_{PV})$, which can be used in the expressions for the power converters. In our case, this first analysis will be based on the buck converter, with the known Eqs. (30)–(32), where V_{bat} = battery voltage (which is assumed with constant voltage for every Δt) and D = duty cycle.

$$I_{PV}(V_{PV}, I_{PV}) = I_L - I_o(e^{(V_{PV}+I_{PV}R_s/mv_t)} - 1) - \frac{V_{PV} + I_{PV}R_s}{R_{sh}}, \tag{29}$$

$$V_{bat} = \frac{t_{on}}{T} V_{PV}, \tag{30}$$

$$P_{in} = V_{PV}I_{PV} = V_{bat}\frac{I_{PV}}{D} = V_{bat}P^*, \tag{31}$$

$$P^*_{Buck} = \frac{I_{PV}}{D}. \tag{32}$$

It can be demonstrated that input power converter, P_{in}, versus duty cycle, D, and P^*_{Buck} versus D present the same maximum points for the same duty cycle values, for constant battery voltage, Fig. 16.

The algorithm, for this method, can be explained as follows: Fig. 17: the tracking process is started with an initial duty ratio. Firstly, the PV current $I_{PV}(t)$ is measured and computed $P^*(t)$. Then, the duty cycle is increased, $\Delta D1$. At stage two, the PV current $I_{PV}(t+\Delta t)$ is measured and computed $P^*(t+\Delta t)$ again. After gathering the past and the present information on the P^*, the controller makes a decision on whether to increase or decrease the duty ration (sign of the incremental duty ratio) depending on the location of the operating point. This tracking process repeats itself indefinitely until the peak power point is reached. The decision is based on the algorithm of Fig. 17 which is the flowchart

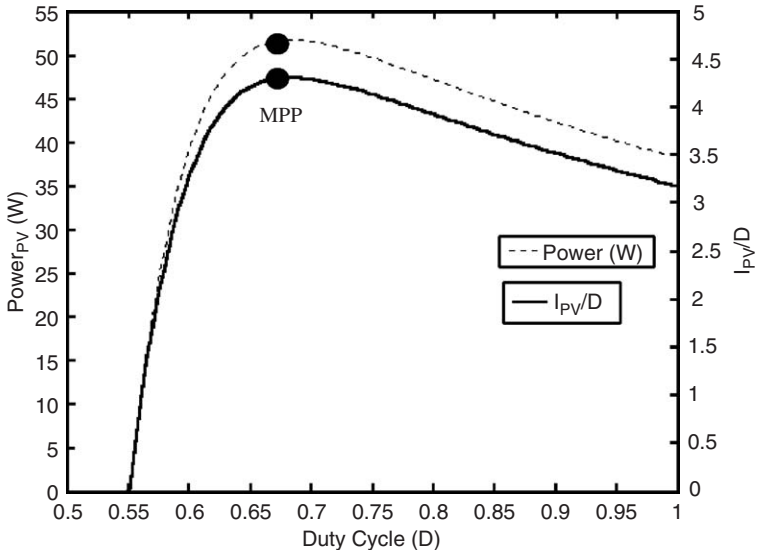

Fig. 16. Simulation results comparing the new algorithm with the photovoltaic power supply [44].

for the peak power tracking control. Then, four cases can be presented, Table 1, where $\Delta P = P^*(t + \Delta t) - P^*(t)$ and $\Delta D = D(t + \Delta t) - D(t)$.

This method has as a major advantage, when compared with other direct methods, the fact that it only uses the measurement of the variable, PV current. In addition, this algorithm operates successfully even in cases of rapidly changing atmospheric conditions and different sky conditions [44,45]. Furthermore, even though this description is made for a step-down DC/DC converter, it can be proven that this method is suitable for any DC/DC topology, step-down and step-up, as is reported in Ref. [44].

2.2.2. *Methods by modulation*

In the methods discussed earlier, the sampling methods, the appropriate adjustment for the maximum voltage point leads a point close to and oscillating around the maximum point. These oscillations are generated automatically by the feedback control used. However, there are many other methods that add an oscillation. These algorithms are known as forced oscillation methods.

2.2.2.1. Forced oscillations methods. Several articles have dealt with this subject [46,47]. For example, Ref. [46] introduces a small voltage, 100 Hz, that is added to the voltage of operation voltage of the PV generator. This leads to a ripple power, whose phase and amplitude are dependent on the relative location of the operation point to the MPP, Fig. 18. If this modulation occurs in zone "A", the left side of the MPP the ripple voltage of the power will be perfectly in phase. However, if the modulation occurs in a point of operation of zone "B", to the right side of the MPP, the curling of the power output will be 180° out of phase with respect to the voltage. In case that the operation point is exactly the MPP, the curling of power output will have twice the frequency of the curling of the voltage, with very small amplitude.

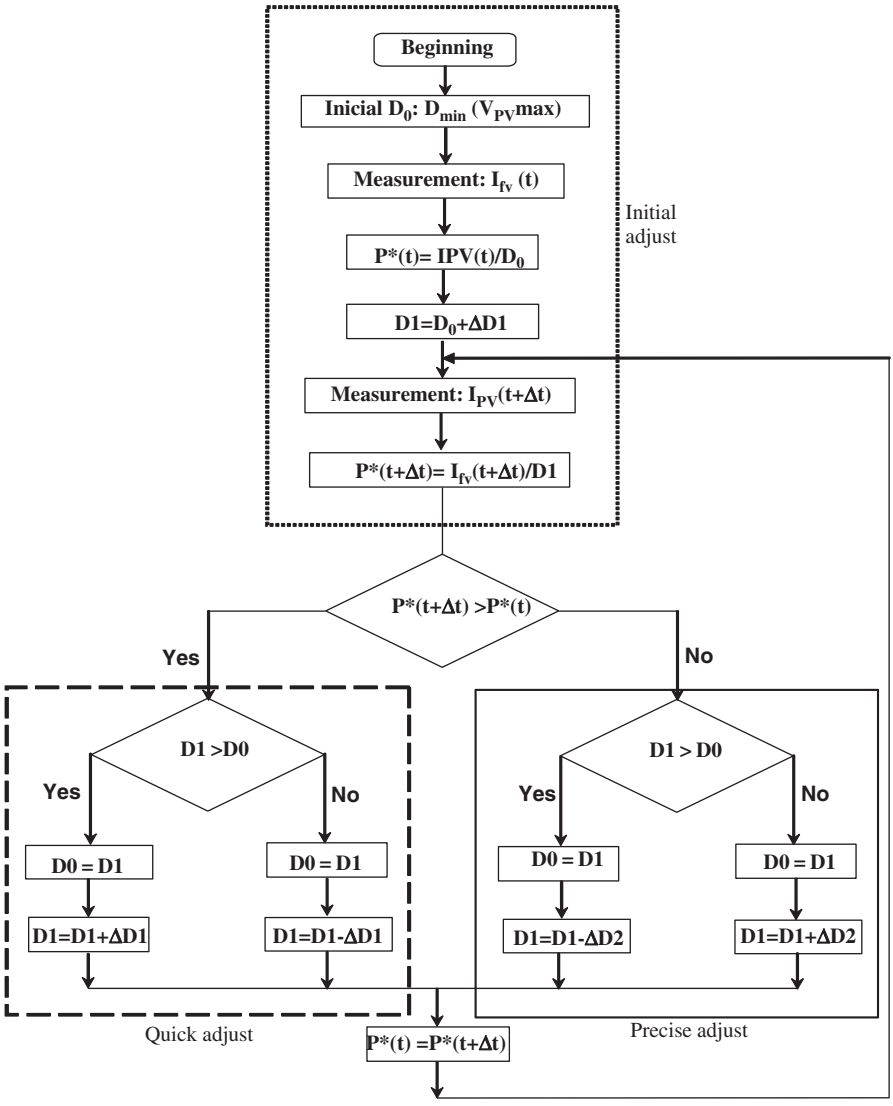

Fig. 17. Flowchart for the algorithm of measurement of the photovoltaic current, I_{PV} [44].

The advantage of this method is that analysis of the amplitude and the phase provides information on the location of the MPP. In addition, the exit signal converges slowly towards zero, when the point of operation approaches the MPP. This allows the operating voltage to be adjusted slowly to the MPP voltage. With it, there will be no continuous oscillation around the MPP caused by a fixed width of passage of converter MPPT. The only oscillation that happens with this method, is 100 Hz of modulation of the voltage operation.

Nevertheless, it has as a disadvantage the greater complexity of its implementation as well as the evaluation of the signals of very low amplitude.

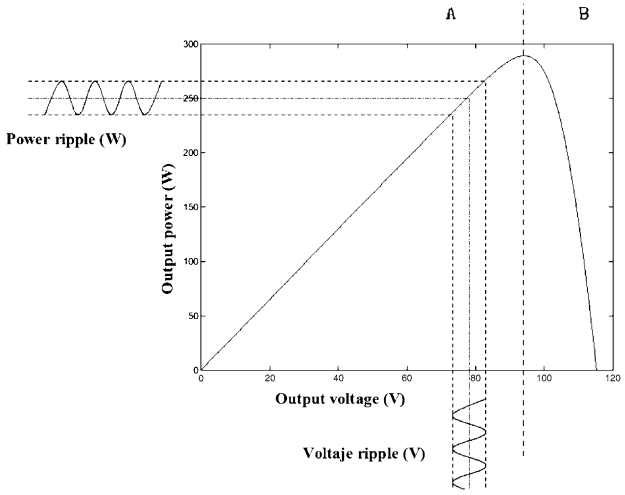

Fig. 18. Curve P–V for a PV generator with the power ripple caused by the photovoltaic voltage modulation. Point "A" denotes the area of operation, on the left of the MPP, and point "B" the area on the right of the MPP.

2.3. Other methods: artificial intelligence methods

In recent years, the fuzzy logic controllers (FLCs) and neural network methods have received attention and increased their use very successfully in the implementation for MPP searching [48–55]. The fuzzy controllers improve control robustness and have advantages over conventional ones. They can be summarized in the following way [47]: they do not need exact mathematical models; they can work with vague inputs and, in addition; they can handle nonlinearities and are adaptative, in nature; likewise, their control gives them robust performance, under parameter variation, load and supply voltage disturbances.

Based on their heuristic nature and fuzzy rule tables, these methods use different parameters to predict the maximum power output: the output circuit voltage and short circuit current [49]; the instantaneous array voltage and current [50–52]; instantaneous array voltage and reference voltage (obtained by an offline trained neural network) [48]; instantaneous array voltage and current of the array and short circuit current and open-circuit voltage of a monitoring cell [53,54] and solar radiation, ambient temperature, wind velocity and instantaneous array voltage and current, used in Ref. [55].

Finally, it is of note that other methods have been implemented such as those that are based on the use of the Fibonacci series [56]. Although, once again, two variables are measured: output voltage and current of the DC/DC converter.

3. Conclusions

In this paper, the state of the art of MPP algorithms has been reviewed. As has been demonstrated, there are many ways of distinguishing and grouping the methods for tracking the MPP to the PV generator. However, in this article the direct and indirect methods were those selected and developed in depth.

The indirect methods (“quasi trackers”) have the particular feature of not obtaining, but rather estimating, the maximum power for either irradiance or temperature. They must measure some of the PV generator’s voltage and current PV (or both), the irradiance or use empirical data, by mathematical expressions of numerical approximations, to estimate the MPP from the specific PV generator installed in the system. Although, in many cases they can be simple and inexpensive, they are not totally versatile with respect to load profile; none of them are able to obtain the MPP exactly, from PV in any atmospheric conditions. Subsequently, they are known as “quasi seeks”.

On the other hand, the direct methods can be also distinguished (“true seeking methods”) which offer the following advantages: neither a large database nor a large memory is necessary for calculating the MPP; they are totally versatile with respect to the load profile; the seeking of MPP is independent of the variation of the parameters of the PV generator. Likewise, the control circuit does not have to be fit for a specific generator, nor must it update when varying their parameters; and it is not necessary to know the level incident irradiance.

Nevertheless, in all direct methods up to now the measurement of the voltage and current of PV generator are required. Notwithstanding, it has been shown that in the direct methods, it is possible to develop a strategy that allows obtaining the MPP by measuring only one variable, the current PV.

Finally, it has been shown that other methods also exist, such as the artificial methods and the Fibonacci series based but two variables must be measured, at least.

References

[1] G. Bopp, H. Galber, K. Preiser, D.U. Sauer, H. Schmidt, Energy Storage in photovoltaic stand-alone energy supply systems, Prog. Photovoltaics: Res. Appl. 6 (4) (1998) 271–291.
[2] J.P. Dunlop, Batteries and charge control in stand-alone photovoltaic systems. Fundamentals and Application, Sandia National Laboratories, 1997.
[3] G.M. Hans, Solar cell and test circuit, Patent US3, 350, 635, 1967.
[4] J.D. Hartman, Power conditioning system, Patent US3, 384, 806, 1968.
[5] T.O. Paine, Maximum Power Point Tracker, National Aeronautics and Space Administration, NASA, Patent US3, 566, 143, 1969.
[6] A.U. Louis, System for detecting and utilizing the maximum available power from solar cells, Patent US3, 696,286, 1972.
[7] M. Togneri, H. Elliott, DC to AC and AC to DC converter systems, Patent, US3,825,816, 1974.
[8] A. Wilkerson, Power maximization circuit, Patent US4,200,833, 1980.
[9] R.H. Baker, US, Method of and apparatus for enabling output power of solar panel to be maximized, Patent 4,375,662, 1983.
[10] K. Nishioka, et al., Analysis of the temperature characteristics in polycrystalline Si solar cells using modified equivalent circuit model, Jpn. J. Appl. Phys. 42 (12) (2003) 7175–7179.
[11] J.C.H. Phang, D.S.H. Chan, J.R. Phillips, Accurate analytical method for the extraction of solar cell, Electron. Lett. 20 (10) (1984) 406–408.
[12] M.A. Hamdy, A new model for the current-voltage output characteristics of photovoltaic modules, J. Power Sources 50 (1–2) (1994) 11–20.
[13] T. Takashima, T. Tanaka, M. Amano, Y. Ando, Maximum output control of photovoltaic (PV) array, Intersociety Energy Conversion Engineering Conference and Exhibit (IECEC), 35th, Las Vegas, NV, July 24–28, 2000, pp. 380–383.
[14] N. Takehara, S. Kurokami, Power control apparatus and method and power generating system using them. Patent US5,654,883. 1997.

[15] H.E.-S.A. Ibrahim, et al., Microcomputer controlled buck regulator for maximum power point tracker for DC pumping system operates from photovoltaic system, Fuzzy Systems Conference Proceedings, FUZZ-IEEE '99, 1999 IEEE International 1 (22–25) (1999) 406–411.
[16] D. Lafferty, Coupling network for improving conversion efficiency of photovoltaic power source, US4,873,480, 1989.
[17] P. Chetty, Maximum power transfer system for a solar cell array, US4,604,567, 1986.
[18] M.A.S. Masoum, et al., Optimal power point tracking of photovoltaic system under all operating conditions, in: 17th Congress of the World Energy Council, Houston, TX, 1998.
[19] M.A.S. Masoum, et al, Design, construction and testing of a voltage-based maximum power point tracker (VMPPT) for small satellite power supply, in: 13th Annual AIAA/USU Conference, Small Satellite, 1999.
[20] J.J. Schoeman, J.D. van Wyk, A simplified maximal power controller for terrestrial photovoltaic panel arrays, IEEE Power Electronics Specialists Conference. PESC '82 Record. New York, NY, 1982, pp. 361–367.
[21] M. Andersen, T.B. Alvsten, 200 W Low cost module integrated utility interface for modular photovoltaic energy systems, Proceedings of IECON '95 1 (1995) 572–577.
[22] M. Abou El Ela, J. Roger, Optimization of the function of a photovoltaic array using a feedback control system. Solar. Cells: Their Science,, Technology, Applications and Economics 13 (2) (1984) 185–195.
[23] S.M. Alghuwainem, Matching of a dc motor to a photovoltaic generator using a step-up converter with a current-locked loop, IEEE Trans. Energy Conversion 9 (1994) 192–198.
[24] T. Noguchi, et al., Short-current pulse-based adaptive maximum power point tracking for a photovoltaic power generation system, Elect. Eng. Japan 139 (1) (2002) 65–72.
[25] J.F. Schaefer, L. Hise, An inexpensive photovoltaic array maximum-power-point-tracking DC-to-DC converter. Number NMSEI/TN-84-1 New Mexico Solar Energy Institute, Las Cruces, New Mexico 88003, Mayo, 1984.
[26] Z. Salameh, F. Dagher, W. Lynch, Step-down maximum power point tracker for photovoltaic systems, Solar Energy 46 (5) (1991) 279–282.
[27] D.L. Lafferty, Coupling network for improving conversion efficiency of photovoltaic power source US4,873,480, 1989.
[28] D. Lafferty, Regulating control circuit for photovoltaic source employing switches, energy storage, and pulse width modulation controller, Patent US5,270,636, 1993.
[29] J.H. David, Power conditioning system, US3,384,806, 1968.
[30] L.T.W. Bavaro, Power regulation utilizing only battery current monitoring, Patent, US4,794,272, 1988.
[31] H.D. Maheshappa, J. Nagaraju, M.V. Murthy, An improved maximum power point tracker using a step-up converter with current locked loop, Renew. Energy 13 (2) (1998) 195–201.
[32] Ch. Hua, Ch. Shen, Comparative study of peak power tracking techniques for solar storage system, in: IEEE Applied Power Electronics Conference and Exposition (APEC'98), vol. 2, 1998, pp. 679–685.
[33] Z. Salameh, D. Taylor, Step-up maximum power point tracker for photovoltaic arrays, Solar Energy 44 (1) (1990) 57–61.
[34] W. Denizinger, Electrical power subsystem of globlastar, in: Proceedings of the European Space Conference, 1995, pp. 171–174.
[35] W.J.A. Teulings, J.C. Marpinard, A. Capel, A maximum power point tracker for a regulated power bus, in: Proceedings of the European Space Conference, 1993.
[36] Y. Kim, H. Jo, D. Kim, A new peak power tracker for cost-effective photovoltaic power systems, IEEE Proc. Energy Conversion Eng. Conf. IECEC 96 3 (1) (1996) 1673–1678.
[37] Ch. Hua, J. Lin, Ch. Shen, Implementation of a DSP-controlled PV system with peak power tracking, IEEE Trans. Ind. Electron. 45 (1) (1998) 99–107.
[38] H. Al-Atrash, I. Batarseh, K. Rustom, Statistical modeling of DSP-based hill-climbing MPPT algorithms in noisy environments Applied Power Electronics Conference and Exposition, 2005. APEC 2005, Twentieth Annual IEEE, vol. 3, 6–10 March 2005, pp. 1773–1777.
[39] K.H. Hussein, I. Muta, T. Hoshino, M. Osakada, Maximum photovoltaic power tracking: an algorithm for rapidly changing atmospheric conditions, IEE Proc. Generation Transmission Distrib. 142 (1) (1995) 59–64.
[40] D.P. Hohm, M.E. Ropp, Comparative study of maximum power point tracking algorithms, Prog. Photovolt: Res. Appl. 11 (2003) 47–62.
[41] X. Liu, L.A.C. Lopes, An improved perturbation and observation maximum power point tracking algorithm for PV arrays, in: Power Electronics Specialists Conference, 2004, PESC 04. 2004, IEEE 35th Annual vol. 3, 2004, 2005–2010.

[42] N. Femia, G. Petrone, G. Spagnuolo, M. Vitelli, Optimization of perturb and observe maximum power point tracking method, IEEE Trans. Power Electron. 20 (4) (2005) 963–973.
[43] A. Branbrilla, M. Gambarara, A. Garutti, F. Ronchi, New approach to photovoltaic arrays maximum power point tracking, in: 30th IEEE Power Electronics Conference, 1999, pp. 632–637.
[44] V. Salas, E. Olías, A. Lázaro, A. Barrado, New algorithm using only one variable measurement applied to a maximum power point tracker, Solar Energy Mater. Solar Cells 1–4 (2005) 675–684.
[45] V. Salas, E. Olías, A. Lázaro, A. Barrado, Evaluation of a new maximum power point tracker (MPPT) applied to the photovoltaic stand-alone systems, Solar Energy Mater. Solar Cells 87 (1–4) (2005) 807–815.
[46] K.K. Tse, H.S.H. Chung, S.Y.R. Hui, M.T. Ho, A novel maximum power point tracking technique for PV panels, in: IEEE Power Electronics Specialists Conference, 2001, PESC. 2001 IEEE, vol. 4, 1970–1975.
[47] A. Cocconi, W. Rippel, Lectures from GM sunracer case history, lecture 3-1: the Sunracer power systems. Number M-101, Society of Automotive Engineers, Inc., Warderendale, PA, 1990.
[48] M. Veerachary, T. Senjyu, K. Uezato, Neural-network-based maximum-power-point tracking of coupled-inductor interleaved-boost-converter-supplied PV system using fuzzy controller, IEEE Trans. Ind. Electron. 50 (4) (2003) 749–758.
[49] B.M. Wilamowski, et al., Microprocessor implementation of fuzzy system and neural networks, in: International Joint Conference on Neural Networks, vol. 1, Washington, DC, 2001, pp. 234–239.
[50] C.-Y. Won, D.-H. Kim, S.-C. Kim, W.-S. Kim, H.-S. Kim, A new maximum power point tracker of photovoltaic arrays using fuzzy controller, in: 25th Annual IEEE Power Electronics Specialists Conference, PESC '94 Record, vol. 1, 1994, pp. 396–403.
[51] A.N. Abd El-Shafy, H.F. Faten, E.M. Abou El-Zahab, Evaluation of a proper controller performance for maximum-power point tracking of a stand-alone PV system, Solar Energy Mater. Solar Cells 75 (3–4) (2003) 723–728.
[52] N. Patcharaprakiti, S. Premrudeepreechacharn, Y. Sriuthaisiriwong, Maximum power point tracking using adaptive fuzzy logic control for grid-connected photovoltaic system, Renew. Energy 30 (11) (2005) 1771–1788.
[53] T. Hiyama, et al., Identification of optimal operation point of PV modules using neural network for real time maximum power tracking control, IEEE Trans. Energy Conversion 10 (1995) 360–367.
[54] T. Hiyama, et al., Evaluation of neural network based real time maximum power tracking controller for PV system, IEEE Trans. Energy Conversion 10 (3) (1995) 543–548.
[55] T. Hiyama, et al., Neural network based estimation of maximum power generation, IEEE Trans. Energy Conversion 12 (1997) 241–247.
[56] M. Miyatake, T. Kouno, M. Nakano, A simple maximum power point tracking control employing fibonacci search algorithm for power conditioners of photovoltaic generators, EPE-PEMC'02, Cavtat & Dubrovnik, 2002.